Flexible Riser Replacement Operation Based on Advanced Virtual Prototyping

Shuai Yuan*, Pierre Major, Houxiang Zhang

Department of Ocean Operations and Civil Engineering, Norwegian University of Science and Technology , Aalesund, Norway

ARTICLE INFO

Keywords:

Flexible riser

Replacement operation

Virtual prototyping

Finite element method

ABSTRACT

As a critical campaign in the offshore oil and gas engineering, flexible riser replacements involve complex operations that need to be optimized and detailed to factor in trends in the industry . Since it allows engineers to interact with simulation tools in real time during the operation design phase, virtual prototyping (VP) is an efficient method to obtain an optimal solution and improve operational procedures in terms of safety and effectiveness for risk-based integrity management of flexible risers. In this study, a real-time VP model is adopted to simulate the process of a water injection flexible riser pulled in from an installation vessel to a jacket platform, which is one of the riser replacements tasks. The results are validated against results based on a finite element analysis. Attention is paid to the configuration, tension, and maximum bending curvature along the flexible riser during the operation. The innovative approach presented in this paper can provide guidance with respect to the operation limitations of a flexible pipe in practical engineering.

1. Introduction

Oil and gas will remain primary energy resources for many years to come (Pedersen, 2015). Flexible pipes have been vital to subsea developments worldwide and to Norwegian oil and gas production facilities since 1986 (Leira, 2015). As shown in Fig. 1, a flexible riser (FR), as a dynamic pipe application, is applied in floating production systems, mainly serving for a high-pressure production, gas lift, and chemical/water injection. According to the Norwegian Petroleum Safety Authority, 326 FRs were in use on the Norwegian Continental Shelf in 2013. However, till 2013, more than 25% of FRs had been replaced due to different failure mechanisms (4Subsea, 2013).

A replacement of FR generally includes two reverse operations, recovery and reinstallation, during which specialized vessels operate in a close range to platforms. Both operations share a high risk of entanglement or spaghetti effect for the risers hung close to neighboring ones, as shown in Fig. 1. In addition, the probability of oil spills increases because replacement operations are typically performed without shutting down field production. Thus, the relevant operations schedule should be carefully designed for FR integrity management based on analyses, experiences, and risk assessments to avoid initiations of failure modes, such as annulus flood, over bending, etc. However, as seen in Fig. 1, the complex unbonded multi-layered structure of FRs not only contributes to the mechanical advantages but also make testing with full-scale physical prototypes highly costly and even unfeasible.

Due to major developments in game engines and performance improvements in both accelerated hardware and real-time compliant mathematical models, up-to-date virtual prototyping (VP) technology can promote safer operation procedures through concept verification, iterative engineering design, crew training, and communication between various teams in a flexible and efficient way, which can be an optimal choice for riser operations optimization. Using advanced VP tools, including ghosting based on real environmental models for wind, waves, and current, allows the visualization of the predicted course of operations during contingency scenarios such as vessel drift-off, crane black-out, riser joint failure, etc. Nevertheless, there is always an issue about the tradeoff between model accuracy and computation efficiency in VP, which makes the validation necessary. To this end, a finite element approach (FEA) model is adopted for the verification purpose in this research since an FEA is a widely accepted tool for the structural analysis of risers (DNV GL, 2018). Compared with VP, a conventional FEA simulation is limited in an offline environment and normally applies to the component analysis in a stress level.

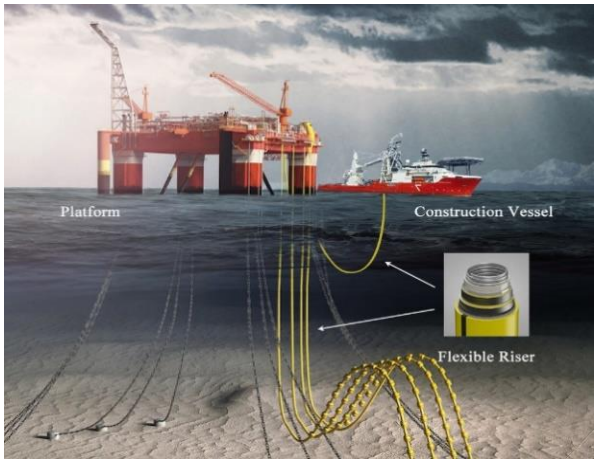

Fig. 1. Typical flexible riser system and cross section (Partly courtesy of Subsea 7)

* Corresponding author. Department of Ocean Operations and Civil Engineering, Norwegian University of Science and Technology, Aalesund, 6009, Norway
E-mail address: shuai.yuan@ntnu.no

The computation, depending on the mesh strategy and the performance of processors, may be tedious and tricky for the simulation of complex operation procedures, which decreases the possibility of effective interactivity. Real-time FEA develops but normally has limited applications (Huang et al, 2015). Compared with the recovery of scrapped risers, greater concern is needed for reinstallation of a new riser, which imposes strict requirements on vessel station keeping capabilities and weather criteria (Fergestad et al, 2014). Thus, the case this paper addresses is an operation for an FR pulled from an installation vessel to a jacket platform. This is the first phase of the reinstallation and in the beginning of this phase the vessel stays most closely to the platform. The general process with 4 selected steps(Step I~IV) for pulling in a riser is shown in Fig.2. The purpose is to identify bottlenecks, such as potential failure possibilities, inconsistencies, and inefficiencies, in the procedures and then optimize the related operation. This paper is extended from Major et al. (2019). An advanced VP framework for the riser operation is applied and the original contribution is integrating virtual reality, real-time and humans in the loop (HITL) into this framework. To assess the VP results in terms of fidelity, FEA correspondingly provides a complete simulation for the consistent procedures. Attention is paid to the equilibrium positions, maximum bend curvature, and axial tension of the flexible riser during the operation.

2. Related works

VP for engineering applications is increasingly developed in maritime industry. Li et al. (2016) presented a VP framework including modeling, simulation, and control for ship maneuvering. Chu et al. (2017) introduced the VP system for maritime crane design and operations. Major et al. (2019) proposed a framework for the study on three positioning solutions of mobile offshore drilling units. Besides, VP is often used with the conjunction of virtual reality and mathematical models for the purpose of training unskilled workers. Zhang et al. (2017) described a mathematical model for virtual reality of a subsea production facilities installation to achieve the training goal. Yu et al. (2017) presented a full mission simulator relying on a similar virtual reality. However, VP has rarely been applied on offshore flexible riser operations. The validation in this paper is implemented for the results calculated by physics module in VP. Lee and Roh (2018) detailed the requirements of physics engines for simulation of shipyard and offshore operations, especially for coupled systems. But the real-time requirement is not fulfilled. Besides, although VP framework for control design is already developed, there is still a lack of the integration capability to interact with HITL and a real-time virtual environment.

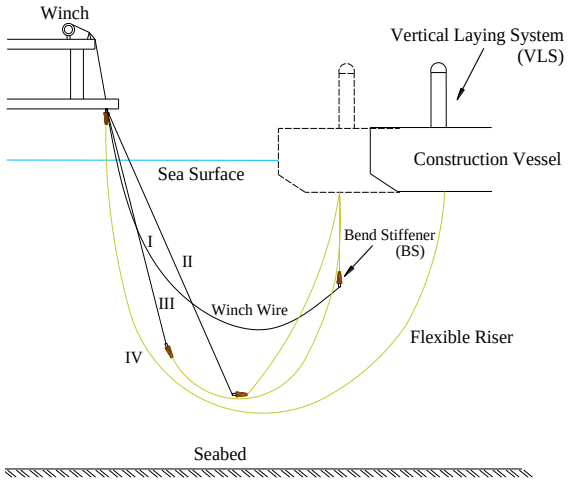

Fig. 2. Schematic representation of riser pull-in operation

Regarding riser operations analysis, advances have mostly been achieved in the research of the structural integrity. For the traditional local failure mechanism study, a 3D finite element model with solid elements was presented in Guedes Mendonça and de Arruda Martins (2017) to investigate the effect of the launching procedure in flexible pipes installation. Collapse performances were experimentally and numerically investigated in Caleyron et al. (2017) to show the installation effect was positive. FEA turns out to be an effective method (Owen and Qin, 1986; Fyling et al, 1998; Chai et al, 2006) in riser global analysis and rod elements (Chen et al, 2011; Ruan et al, 2017) or beam elements (Guo et al, 2018) have often been adopted for the modelling of risers. In addition to common wave configurations, Amaechi et al, 2019 carried out the dynamic analysis on hoses in the Chinese-lantern configuration attached to a Catenary Anchor Leg Moorings buoys. RAO was acquired by ANSYS AQWA and coupled dynamic mode was developed by Orcaflex. Besides, Chrolenko et al. (2013) developed a dynamic analysis model of which installation vessel was coupled with the riser system used it to assess risk and weather limitations for riser replacements. The boundary control problem of a marine flexible riser installation system was investigated in He et al. (2013) with numerical simulations. In addition, as an alternative solution to pipeline installation planning and decision making, a real-time offshore pipeline installation monitoring system was developed. (Wang et al, 2017) The realistic pipeline behavior is calculated by Orcaflex based on data acquired from sensors.

3. Flexible riser pull-in operation

3.1. Operation introduction

Riser replacement operations are complex and perilous when the production platform is connected to multiple risers. The object here is a single water-filled FR operated in shallow waters. The whole pull-in procedure in this case includes 14 steps which are simulated in VP and FEA, respectively. A general introduction is as follows, starting with the initial conditions of this procedure, which is depicted in Fig.3:

1). Offshore vessel equipped with VLS mounted over a moonpool stays in close range to the platform, using Dynamic Positioning (DP) to keep the position and heading.

2). Offshore vessel pays out part of the riser by tensioners through the moonpool center (point *A*).

3). An end of the winch wire on the platform is connected to the riser topside termination, which is protected by a bend stiffener (BS) against over bending/fatigue damage.

In the following operations, keeping the heading always restricted, VLS pays out the riser by different lengths in the subsequent steps while the platform winch hauls in the wire to receive the riser. The vessel moves away from the platform in certain steps without paying out or hauling in. The pull-in operation finishes when the topside termination reaches the platform and is installed to the locking mechanism on the platform.

The steps above are designed to avoid the potential risks during the operation, e.g. the collision between the vessel and platform, the collision between the riser and the moonpool's wall, or the jackets' legs or seabed and the excessive stretches on the riser and winch wire. Thus, the riser/winch wire configurations, tension and curvature during the operation should be analyzed for the validation.

3.2. Simplified mechanical analysis

During a general pull-in operation, the riser and winch wire both experience large displacements and rotations under dynamic boundaries in reeling process and dynamic environment loads, which makes these flexible slender structures show strong geometrically nonlinear dynamic behaviors. For the numerical method in the riser mechanical analysis, the results derived from classic catenary theory is often adopted as initial iteration value for the following mechanical analysis. Therefore, as a beginning work of the whole operation study, a simplified mechanical analysis for initial static configuration is shown in this section based on classic catenary theory. As shown in Fig.3, the focus is on *AB* part which includes 3 sections: *AE* (riser), *ED* (BS), and *DB* (wire). The initial equilibrium configuration is subjected to the distributed gravity/buoyancy and support tensions. By neglecting the bending stiffness and axial strain, *AE* and *DB* are both simplified as catenaries in the two-dimensional *XZ* plane while *ED* is considered as a rigid straignt line. The known variables are the lengths of three parts L_{AE} , L_{ED} , L_{DB} , vertical distance V_{AB} and horizontal distance H_{AB} , and equivalent weights per length ρ of each part. The buoyancy from the seawater should be taken into account for ρ of the parts in the sea(*FE*, *DI*, and *IC*). Based on the catenary theory, Equations (1)~(8) can be obtained. *AF*, *FE*, and *CB* are all catenary parts without the lowest point and provide similar equations..

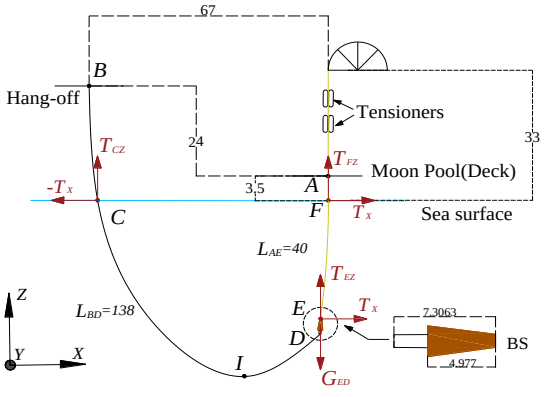

Fig. 3. Initial Configuration of Pull-in Operation (unit: m)

$$V_{ij}=\frac{1}{\rho_{ij}g}\left(\sqrt{T_{iZ}^2+T_X^{\ 2}}-\sqrt{T_{jZ}^2+T_X^{\ 2}}\right) \tag{1}$$

$$H_{ij}=\frac{T_X}{\rho_{ij}g}\left[\sinh^{-1}\left(\frac{T_{iZ}}{T_X}\right)-\sinh^{-1}\left(\frac{T_{jZ}}{T_X}\right)\right] \tag{2}$$

Where, $i=A,F,C$ and $j=F,E,B$, respectively. The projection lengths of parts on the *Z* axis is V and the *X* axis is H . T_Z is the force component along the *Z* axis while T_X is the force component along the *X* axis. *DI* and *IC* parts have the lowest points included. Thus, the vertical projections of *DI* and *IC* can be presented in the following.

$$V_{DI}=\frac{T_X}{\rho_{DC}g}\left(\cosh\frac{H_{DI}\rho_{DC}g}{T_X}-1\right) \tag{3}$$

$$V_{IC}=\frac{T_X}{\rho_{DC}g}\left(\cosh\frac{H_{IC}\rho_{DC}g}{T_X}-1\right) \tag{4}$$

The initial payout lengths of riser (*AE*) and wire (*DB*) are expressed as:

$$L_{AE}=L_{AF}+L_{FE} \tag{5}$$

$$L_{DB}=\frac{T_X}{\rho_{DC}g}\cdot\sinh\frac{H_{DI}\rho_{DC}g}{T_X}+\frac{T_X}{\rho_{DC}g}\cdot\sinh\frac{-H_{IC}\rho_{DC}g}{T_X}+L_{CB} \tag{6}$$

Where, L is the length of each part. The vertical force components at point *A*, *B*, *C*, *D*, *E*, and *F* are calculated by the gravities below the points, respectively. Catenary equations are only used for *DI* and *IC* parts. Take point *C* and *F* as examples to show as:

$$T_{CZ}=T_X\cdot\sinh\frac{-H_{IC}\rho_{DC}g}{T_X} \tag{7}$$

$$T_{FZ}=\rho_{FE}g\cdot L_{FE}+T_X\cdot\sinh\frac{H_{DI}\rho_{DC}g}{T_X}+G_{ED} \tag{8}$$

G_{ED} represents the equivalent weight of the BS. Another 4 equations for point *A*, *B*, *D*, and *E* can be similarly obtained as well. According to the equilibrium of the moment at point *D* and the geometric relationship of BS, the following equations can be obtained:

$$T_{EZ}\cdot H_{ED}+G_{ED}\cdot H_{ED}/2-T_X\cdot V_{ED}=0 \tag{9}$$

$$H_{ED}^2+V_{ED}^2=L_{ED}^2 \tag{10}$$

The whole system should satisfy the compatibility. Therefore, there comes:

$$H_{AB} = -H_{IC} + H_{CB} + H_{DI} + H_{ED} + H_{FE} + H_{AF} \quad (11)$$

$$V_{AB} = V_{CB} + V_{IC} - V_{DI} - V_{ED} - V_{FE} - V_{EA} \quad (12)$$

As explained, Equations (1)~(12) can be extended to 20 equations in total for the whole *AB* part that can lead to 20 unknowns($T_{AZ}, T_{BZ}, T_{CZ}, T_{DZ}, T_{EZ}, T_{FZ}, T_X, V_{DI}, V_{IC}, V_{FE}, V_{ED}, L_{CB}, L_{AF}, L_{FE}, H_{AF}, H_{FE}, H_{CB}, H_{DI}, H_{IC}, H_{ED}$) determined by built-in method vpasolve in Matlab. The initial equilibrium position of *AB* part then can be obtained and will be discussed in Section 6.2.

4. Advanced virtual prototyping

4.1. Software Architecture

The virtual prototyping work is implemented by the Offshore Simulator Centre (OSC), Norway. The architecture of the software adopted for VP is illustrated in Fig.4. The Sandbox is the instructor module, which starts and controls the simulation scenarios. In the platform called Fathom which is developed by OSC, the Core is the central module that dispatches the commands and feedbacks to the various modules, e.g. communicating with physics engines via the APIs (JNI), and with the Sandbox (two ways) and visual channels (one way) via a gaming network middleware called RakNet. The visual channels can update the visual frames (FPS) faster than the network update rate using interpolation, which smoothes network jitters. The Physics is a general-purpose physics solver that assesses the behaviors of flexible slender bodies and rigid bodies in different scenarios. It is implemented in AGX Dynamics, which offers a mix of solvers suitable for iteration on fast approximate solutions and runs at 60Hz. The Visualization, implemented on a game engine platform with broad developer base called Unity, provides a life-like immersive environment. In addition, the Human Machine Interface (HMI) developed in Fathom with JavaFX sends the winch/vessel lever commands from the human experts who perform the simulation. Therefore, the framework can be used to identify bottlenecks and possible human communication challenges between the various teams during the simultaneous operations (SIMOPS) such as an offshore operation manager, winch/reel operator, remotely operated vehicle pilot, and offshore vessel captain.

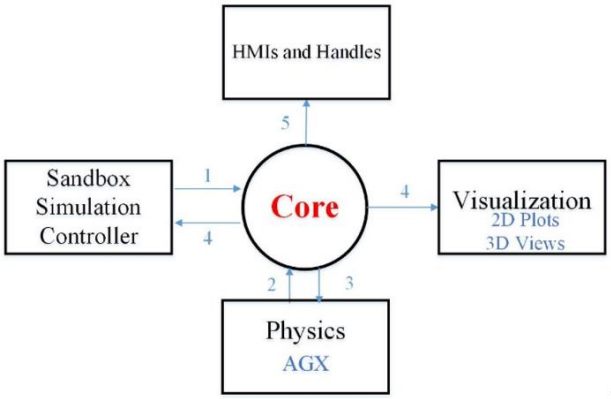

Fig. 4. Sandbox Framework Architecture

4.2. Communication between modules

According to the VP framework, the user firstly starts with Sandbox and chooses a scenario. Then the core is initiated with the set environmental parameters such as wind, wave, and current settings. Following the numbering in Fig. 4, the communications between modules are as follows.

1. Core module starts the simulation and obtains the commands from Sandbox.
2. Core sends the environmental conditions, forwards the commands to Physics, which calculates the forces, accelerations, velocities, positions, and orientations of all objects in the scene.
3. Results obtained are forwarded back to Core.
4. Core forwards the positions and orientations to Visualization at 60 Hz and sends the static and dynamic properties of all the objects in the simulation to the Sandbox
5. for the purpose of logging and analysis.
6. The HMI module transfers the commands from the winch operators to the Core module.

4.3. Physical Model

A scene is a description of how the models are interconnected and how they behave. All scene items are placed and connected in a Fathom module dedicated to composing scenes in a 3D environment, which avoids time-consuming and error prone XML tree structure editing of scene configuration.

The physical properties of the main components in the model are listed in Table 1. In AGX, the FR and the winch wire are both modeled by AgxWire, which is a hybrid multiresolution wire combining lumped elements and massless quasi-static representations without torsional properties. The lumped element resolution is adapted dynamically based on local stability criteria, which means the mesh density is changeable during the simulation. The tensioner is modeled as a winch in

Table 1.
Sandbox Model Properties

Component	Property	Value
Flexible Riser	Water filled density (kg/m^3)	2235
	Outside diameter (m)	0.2359
	Linear density (kg/m)	102.1
	Bending modulus (Pa)	9.904E7
	Tensile modulus (Pa)	3.25E10
Winch Wire	Density (kg/m^3)	7800
	Diameter (m)	0.030
	Linear density (kg/m)	5.50
	Bending modulus (Pa)	1E9
	Tensile modulus (Pa)	1.5E11
Ancillaries	Bending modulus	Rigid body
	Volume (m^3)	2.1
	Dry weight (kg)	4382
Others	Water density (kg/m^3)	1080
	Water depth (m)	75
	Original line resolution (points per meter)	4

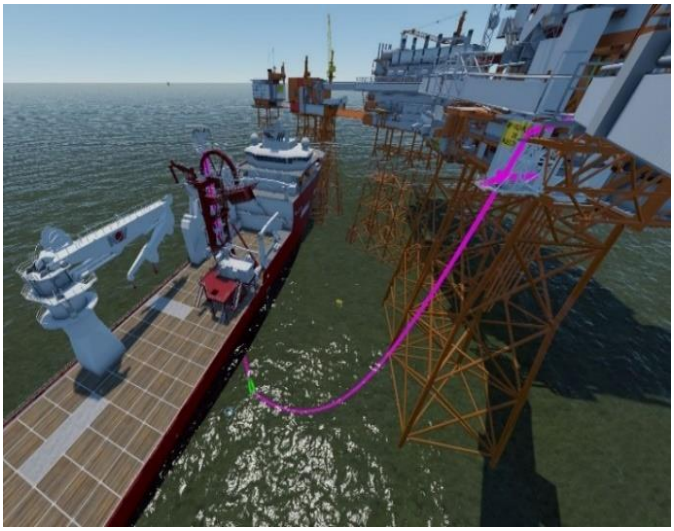

Fig. 5. Step 0 of the pull-in operation for a flexible riser

the 3D model of the vessel. The platform winch is placed at the relevant position on the deck. Both winch drums are not modeled, which gives a significant performance boost without sacrificing precision. The vessel is modeled with a DP system that controls the vessel's heading and position during offshore operation. To circumvent a limitation of AGX not handling the buoyancy of the riser properly, the water density is chosen to be at 1080 kg/m^3. Fig. 5 shows the visualization result of the simulation for Step 0. The green highlight line represents the BS. The purple highlight line that is divided by the green line represents the flexible riser between the vessel and the BS and the winch wire from the BS to the platform.

4.4. Logged information

The logging or data acquisition is performed at predefined operational steps. The logged tension data comprises tension along the riser and tension along the wire based on simulation time and procedural steps. As mentioned, Agxwire has dynamic resolution. For calculation stability, the higher the tension is, the coarser the resolution becomes. Therefore, not every position along the riser/wire has a continuous data during the simulation. The winches are commanded by operators with the help of joystick. As preventing excessive riser bend is a key to operation, the position with minimal radius of curvature is added to the logs for the validation.

5. Validation based on FEA

5.1. FEA-based Modeling

To validate the results from VP, an FEA-based simulation is adopted for the pull-in operation of a flexible riser. As an initial study, a calm environment, e.g. static sea state, is set for the verification work. Therefore, due to the low speed operation and static environment, the pull-in operation case can be regarded as a nonlinear static process without considering inertia effect and the flow effect from seawater. Followed by the operation procedure and the physical model presented in Section 3 and 4, basic four parts (FR with BS, winch wire, two drums) are introduced in the FEA model created with the commercial software suite ABAQUS 2019. This general FEA suite consists of modeling, simulation, and visualization for event-based realistic analysis. The configuration, tension, and bending radius along the flexible riser can be calculated after the system meets the compatibility and equilibrium requirements. Besides the parameters in Table 1, the additional parameters for FEA are shown in Table 2.

1) *Flexible riser*

According to the nominal bending stiffness and axial stiffness, the equivalent geometry and material for the cross section of the riser can be obtained to create the riser model using beam elements which are suitable for the riser global analysis. In this case, the hybrid beam elements are adopted because they well handle the slender structures which have significant axial stiffness compared to the bending stiffness. The axial force is treated as an independent unknown introduced in the internal virtual work (Dassault, 2019), as follows.

$$\delta W = \int_L (\tilde{N}\delta\varepsilon + M\delta\kappa + \delta\lambda(N - \tilde{N}))dL \tag{13}$$

Where, W is the internal virtual work, L is the length, N is the axial force variable and $\tilde{N}$ is the independent variable, $\delta\lambda$ represents a Lagrange multiplier imposing $N = \tilde{N}$, M is the force moment, and κ is the curvature of the cross section. The hybrid beam element B31H with 2-node linear beam in 3D space is introduced to model the flexible riser from moonpool level (point *A* in Fig. 3) to BS's tip end (point *E* in Fig. 3), which is a free hanging part. The model adopts 949 elements in the mesh strategy. For the efficiency and comparison with VP, mesh density is generally defined as 4 nodes per meter while the mesh density is increased as 10 nodes per meter in the region of 20 m near BS which considers the convergence and accuracy.

2) *Ancillaries*

This part is extended from the riser and consists of the BS, pup piece, end fitting, and pull head. Since this part is simplified as a rigid body in the VP model, it is also modeled as a rigid body in FEA. The encased riser section is considered in the gravity of this part.

3) *Winch wire*

The part between the actual position of winch drum and hang-off position has been ignored for simplicity. As a slender structure, the winch wire also adopts B31H elements with equivalent bending stiffness and the same mesh density (4 nodes per meter) as the riser. A joint without rotation restrictions is

Table 2.

Additional Parameters for FEA

Property	Value
Total paid-out riser length (m)	214.6
Total hauled-in wire length (m)	138
Drum radius (m)	6
Drum width (m)	1.5

created for the hinge between the wire and pull head to retract the riser.

4) *Reeling systems*

Two reeling systems in the operation are both simplified as simple drum shapes and simulated as rigid bodies in the model. The reference point representing rigid body is set in the center of each drum. The top end points of riser and wire are coupled with the reference points, which means all the degrees of freedom for end points are consistent with reference points. The contact and separation in the interactions between drums and slender structures are using surface-to-surface formulation in the frictionless contact pairs.

5) *Environment*

According to the benign environment of the project, only the buoyancy is considered for this simulation. ABAQUS Aqua is a module used to apply buoyancy, steady current, wave, and wind loading to the model. This module is introduced to the model by editing keywords in the input file.In the Aqua module, the buoyancy is calculated based on the real volume of each component in the sea.

5.2. FEA-based simulation for operation

The procedure of FEA simulation consists of position initialization, riser pay out, wire haul in, and vessel translation. These steps are all set as static analysis, which means the inertia effect is excluded. In the simulation, evenly reeling on and off the drums for the winch wire and riser are controlled by the displacements of top end points and the normal contact introduced by the drums rotating around the Y-axis in Fig. 3 and translating along the Y-axis. In addition, the freedom of the joint between the wire and pull head is restricted along the Y-axis to prevent the riser/wire from touching themselves on the drum. An implicit method is adopted although it involves convergence issue. This usually takes longer time to complete, compared to the explicit method but leads to more accurate results. The FEA simulation on this research work was run on an i7-4770@ GHz CPU.

1) *Initialization*

A schematic of the initial configuration of pull-in is shown in Fig. 3, which shows the initial length and spatial relations of components in the system. Since the accurate initial configurations under environmental loads are indeterminate in the preprocessing of this general-purpose software, three steps below are adopted for the initialization.

Step 1: Fig. 6 (1) shows the condition without environmental loads. Two reference points are both fixed. The spatial relation is kept based on the horizontal distance 67m. The blue line represents the winch wire with original length while the yellow line represents the riser.

Step 2: The gravity is applied on the wire and riser. The riser is reeled on the drum by the drum rotating and lowering down with the rest paid out length reaching the predefined value after the initialization as shown in Fig. 6 (2).

Step 3: The winch drum is lowered down to the actual position, pictured in Fig. 6 (3,4) as the final step of initialization.

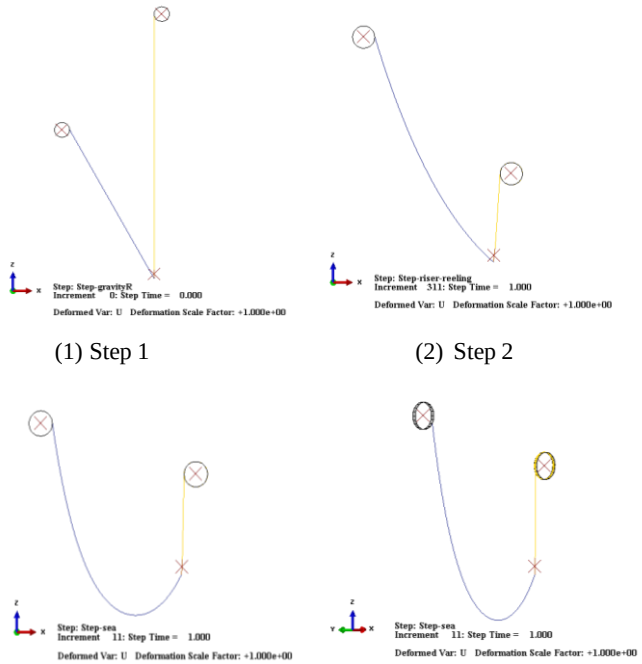

(1) Step 1 (2) Step 2

(3) Final-front view (4) Final-iso view

Fig. 6. Steps for initialization stage

2) *Pull in*

According to the designed operation procedures, the first step is simultaneously paying out the riser and hauling in the winch wire. Then, the pay out, haul in, and vessel translation are operated alternately. The whole simulation is conducted in a continuous way, which means the results of each step will have impact on the next step in terms of stress analysis.

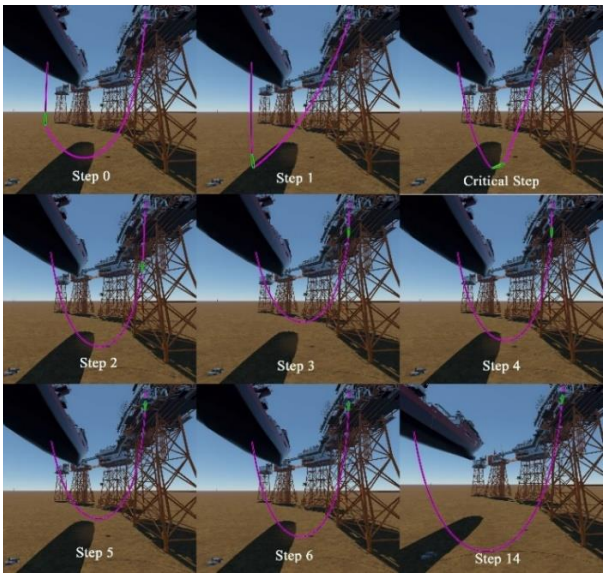

Fig. 7. Operation results of Step 0 -Step 14 from VP (Except Step7-Step13)

6. Results and discussions

In order to verify the virtual prototyping by the difference of these two methods, comparisons are made between the results obtained from the VP simulation and from FEA.

6.1. Sandbox Results

The operation was run on a standard gaming machine with an i7-6700K @4Ghz CPU and could be performed at a real time factor of 2, which means that the simulation time goes twice as fast as the wall clock time. As a result, the simulation starts from Step 0, as pictured in Fig. 7 with the riser hanging vertically and stops at Step 14. The critical step when the largest curvature of riser is reached is shown as Critical Step in Fig. 7. The oreintation of BS is nearly horizontal. Step 0-Step 5 are steps for the completion of BS hanging on and then Step 6-Step 14 are adopted for the rest procedures to find a suitable hanging position for the riser in case of touching down the seabed. For simplicity, Step 7-Step 13 are not shown in Fig. 7. The seawater is not rendered for the sake of scenario visibility. For different conditions, the whole riser points positions are stored.

6.2. Configurations in the pull-in process

As mentioned, during the operation in the subsea, the configurations of these slender structures should be well predicted to avoid collisions with other objects in the process. The coordinates for the riser and winch wire in the VP model are based on the actual positions in the scene, while there are no requirements for the absolute positions of the objects in FEM. Thus, the simulations in the VP and FEA don't need to stay in the same plane. Here the configurations are studied based on the arc length to eliminate the impacts of orientations.

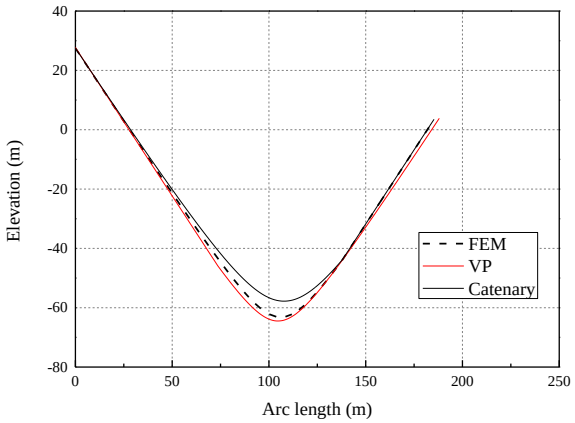

(a) Initial elevations of riser/wire

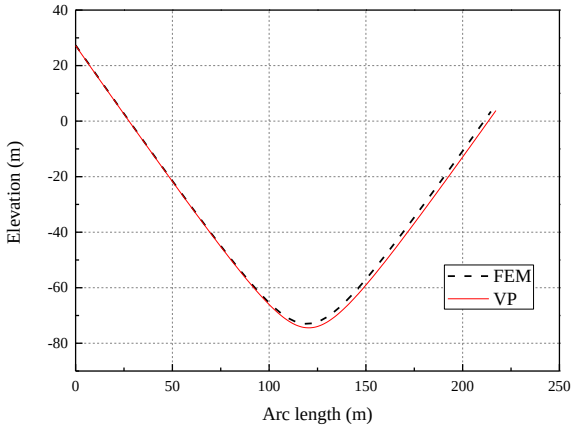

(b) Final elevations of riser/wire

Fig. 8. Elevations based on different methods

Fig. 8(a) shows the comparison of the initial configurations of riser and wire in 3D space while Fig. 8(b) presents the final configurations. The positive direction of *X* axis indicates the increase of arc length from point *B* to point *A* in Fig. 3. From the curves in the figures, the variations of the elevation from initial condition to the final condition are generally similar for different methods. In Fig. 8(a), the results from Section 3.2 have been compared with FEM and VP. The coordinate of lowest point (107.8, -61.3) from catenary method ishigher than FEM (106, -66.7) and VP(104.7, -68). The differences for elevations are both within 11%, which results from the assumptions in the catenary method. Besides, it is noticed that the agreements between the configurations from FEA and VP in these two steps are basically good.

6.3. Tensions at measure points.

The maximum allowable tension is considered as an important design criterion for the winch or tensioner capacity in the installation process. However, due to the dynamic resolution of Agxwire, fixed points for logging the tension are limited. Therefore, the measure points are chosen at moonpool (MT) and the hook between BS and wire (HT). In Table 3, the results from 14 steps correspond with Fig. 7. The error is set as an absolute value. It can be clearly seen that the differences for the riser tension between VP and FEA at most of the steps are within 6% except Step 0, which means the tension of riser from VP are acceptable in these steps. For the tension of hook, the errors in the most of steps are within 10% except Step 0 and Step 1. The most of differences probably results from different

Table 3.

Tensions at the measure points

	MT (t)			HT(t)		
Step	VP	FEA	Error	VP	FEA	Error
0	5.6	5.0	12%	0.35	0.14	1.6
1	6.27	5.93	5.71%	0.24	0.11	1.3
2	4.53	4.60	1.51%	5.97	5.50	8.47%
3	3.73	3.85	3.19%	9.32	8.94	4.20%
4	4.24	4.42	3.98%	9.83	9.47	3.85%
5	3.90	4.07	4.13%	10.8	10.44	3.41%
6	4.50	4.60	2.17%	11.4	10.98	3.83%
7	4.53	4.63	2.16%	11.4	11.00	3.63%
8	5.04	5.12	1.64%	11.9	11.55	3.03%
9	5.07	5.16	1.65%	11.9	11.57	2.84%
10	5.09	5.17	1.64%	11.9	11.59	2.71%
11	5.19	5.31	2.17%	12.1	11.72	3.26%
12	5.22	5.33	2.00%	12.1	11.73	3.13%
13	5.31	5.46	2.70%	12.2	11.86	2.83%
14	5.43	5.42	0.18%	12.4	11.93	3.12%

modelling methods in VP and FEA. In VP, for example, the reeling process has been simplified by paying out different

riser/wire lengths while in FEA the reeling has been simulated by a dynamic boundary that rotates with a drum and it is a continuous iterative process, which is closer to the reality. In addition, HT obtained from Section 3.2 for Step 0 is 0.19t which is much closer to FEA than VP. Thus, the large differences in the initial steps indicate that the differences between FEA and VP have a big impact especially on the initial small HT (equivalent

weight of wire) and should be improved.

6.4. Curvature variation at BS's tip end

Excessive bending can lead to local buckling of the flexible riser. According to API 17J (2014), the minimum bend radius is from the concepts of minimum storage radius and the minimum locking radius. Fig. 9 shows the configurations when the maximum curvature happens. (See Fig. 9(a) for the VP result

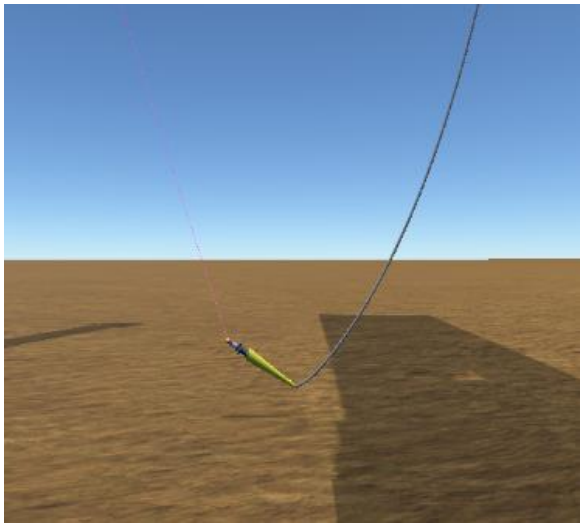

(a)Detail view of VP model

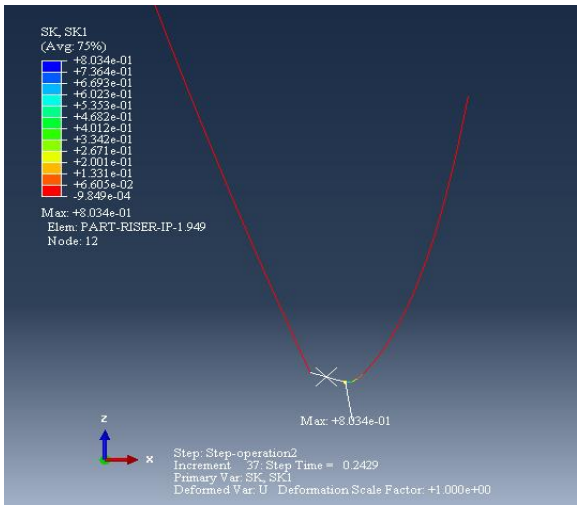

(b)Detail view of FEM

Fig. 9. Bending near BS's tip end at critical moment

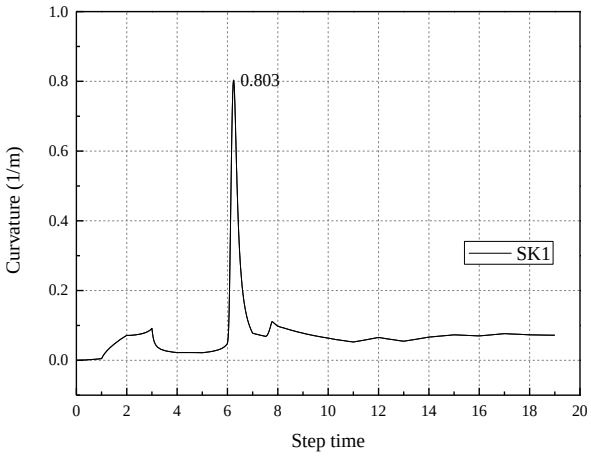

Fig. 10. Curvature of the BS's tip end from FEA

and Fig. 9(b) for the FEA result.) Since the BS is modeled as a rigid body both in VP and FEA, there is a sharp change at the connection between BS and riser. SK1 is the component of section curvature around the main normal exported from ABAQUS, indicating that the location of maximum curvature is at the end of FR which is represented by BS's tip end in this section. For further study about the curvature variation, Fig. 10 shows the curvature of the BS's tip end at all the steps while Fig. 11 presents the curvature variation from BS to riser at the critical step based on Equation (14), which is according to the differential geometry,

$$\kappa = \frac{|\dot{r} \times \ddot{r}|}{|\dot{r}|^3} \tag{14}$$

Where, r is the position on the riser, $\dot{r}$ is the change rate of directions between 2 consecutive points, $\ddot{r}$ is the change rate of 2 consecutive changes of directions, and κ is the curvature at that position. The maximum curvature happened at the same position (BS's tip end) in the simulations of FEA and VP. The peak values are also similar in terms of the error 3%. In addition, the reason for the different critical curvatures between ABAQUS and Equation (14) is that the former is calculated based on the cross-section properties and the Equation (14) is

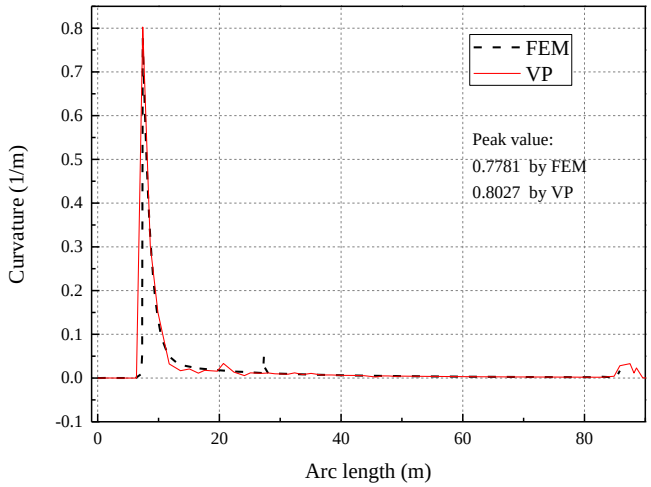

Fig. 11. Curvature variation along the riser length

according to the curve properties in terms of differential geometry without cross-section properties. According to the critical curvature, the real tapered bending stiffness of BS should be taken into account in both simulation and real practice to avoid local buckling at the connection.

7. Conclusions

As a critical activity during the replacement of an FR, the pull-in procedure for a flexible pipe transferred from an installation vessel to a jacket platform is studied in this paper. The results obtained from the virtual prototyping framework are compared with the ones achieved from the finite element simulation. With the whole procedure modeling, the changes of configuration, tension, and curvature of the riser section are mainly studied in detail. The two sets of results are basically in a good agreement, and it can be concluded that:

1). The virtual prototyping model is physically suitable for predicting the riser behavior. Consistent procedure can predict the mechanical variation at any time in the process of operation.

2). Simulating winches without reels in the virtual prototyping framework did not affect the accuracy of the tension at either end in the most steps.

3). Modeling the BS as a rigid object coating the riser is a conservative approach, since it tends to overestimate the curvature of the riser at its open end.

4). The limitation from the capabilities of hardwares adopted have little impact on the case study since the real time requirement has been reached.

This work is suitable for any flexible slender structure in the offshore pull-in operation, for example, cable, umbilical, etc. However, the operation in this simulation is a comparatively simple case. Future work should be extended to apply more severe dynamic environmental loads and boundary conditions. This implies the requirement of considering the vessel model with Response Amplitude Operator from a hydrodynamics analysis tool such as Wamit or ShipX. The comparison with ABAQUS will then be based on statistical estimates of multiple runs. Once the dynamical analysis is validated, it will be possible to conduct virtual prototyping of the riser installation operation with crews improving procedures by avoiding collisions and over bending within the weather window.

Acknowledgment

We appreciate Aker Solutions Visioneering and Subsea7 for the inputs. We are grateful to the Research Council of Norwayfor financing the MAROFF research project under the “Riser Operation Replacement Optimization” Grant 282398. We also thank Mathieu Edet, Inge Blaalid, and Martin Ferstad Aasen from the Offshore Simulator Centre for their efforts on the virtual prototyping framework.

References

API 17J. 2014. Specification for unbonded flexible pipe[S]. Washington，DC: American Petroleum Institute.

Amaechi, C. V., Wang, F., Hou, X., & Ye, J., 2019. Strength of submarine hoses in Chinese-lantern configuration from hydrodynamic loads on CALM buoy. Ocean Engineering, 171, 429-442

Algoryx Simulation AB: AGX Dynamics, 2020. [accessed 2020 March 20] https://www.algoryx.se/documentation/complete/agx/tags/latest/UserManual/source/index.html

Chu Y, Hatledal, L.I., Zhang H, Æsøy V and Ehlers S. 2017. Virtual Prototyping for Maritime Crane Design and Operations, Journal of Marine Science and Technology.

Caleyron, F., Le Corre, V. and Paumier, L., 2017, September. Effect of Installation on Collapse Performance of Flexible Pipes. In ASME 2017 36th International Conference on Ocean, Offshore and Arctic Engineering. American Society of Mechanical Engineers Digital Collection.

Chai, Y.T., Varyani, K.S., 2006. An absolute coordinate formulation for three dimensional flexible pipe analysis. Ocean Eng. 33 (1), 23–58.

Chen, H., Xu, S., Guo, H., 2011. Nonlinear analysis of flexible and steel catenary risers with internal flow and seabed interaction effects. J. Mar. Sci. Appl. 10 (2), 156–162.

Chrolenko M, Gundersen G, Eikanger T E, et al.,2018. Fully Coupled Time Domain Simulation Model Used for Planning and Offshore Decision Support During Riser Replacement Operations[C]//ASME 2018 37th International Conference on Ocean, Offshore and Arctic Engineering. American Society of Mechanical Engineers: V001T01A070-V001T01A070.

Dynamic risers, 2018. Standard DNVGL-ST-F201, DNV GL Høvik,

4Subsea, 2013. Un-bonded flexible risers - recent field experience and actions for increased robustness. Technical report, 4Subsea.

Fergestad, D., Løtveit, S.A., 2014. Handbook on Design and Operation of Flexible Pipes, NTNU, 4Subsea and MARINTEK.

Fylling, I., Larsen, C.M., Sødahl, N., Passano, E., Bech, A., Engseth, A.G., Lie, E., Ormberg, H., 1998. Riflex user’s manual. Marintek Report, Trondheim, Norway.

Guedes Mendonça, H. and de Arruda Martins, C., 2017, September. Parametric Analysis of Crushing and Squeezing Loads Over a Flexible Pipe During Installation Procedure. In ASME 2017 36th International Conference on Ocean, Offshore and Arctic Engineering. American Society of Mechanical Engineers Digital Collection.

Guo, S., Li, Y., Li, M., Chen, W. and Kong, Y., 2018, September. Dynamic Response Analysis on Flexible Riser With Different Configurations in Deep-Water Based on FEM Simulation. In ASME 2018 37th International Conference on Ocean, Offshore and Arctic Engineering. American Society of Mechanical Engineers Digital Collection.

Huang, J.M., Ong, S.K. and Nee, A.Y., 2015. Real-time finite element structural analysis in augmented reality. Advances in Engineering Software, 87, pp.43-56.

Hye-WL, Myung-Il R, 2018. Review of the multibody dynamics in the applications of ships and offshore structures, Ocean Engineering, Volume 167, Pages 65-76, ISSN 0029-8018

He W, Zhang S, Ge S S. 2013. Boundary control of a flexible riser with the application to marine installation. IEEE Transactions on Industrial Electronics, 60(12): 5802-5810

Leira, B., Berge, S., Løtveit, S.A., Fergestad, D., Langhelle, N., 2015, May. Lifetime extension of flexible risers: a generic case study. In: Offshore Technology Conference. Offshore Technology Conference.

Li G, Skogeng PB, Deng Y, Hatledal LI, and Zhang H. 2016. Towards a virtual prototyping framework for ship maneuvering in offshore operations. In IEEE OCEANS 2016-Shanghai, p. 1-6

Major P, Skulstad R, Li G, Zhang H., 2019. Virtual prototyping: a case study of positioning systems for drilling operations in the Barents Sea, Ships and Offshore Structures

Major, P., Yuan, S., Zhang, H., Blaalid, I., Edet, M., & Ferstad, M. (2019, June). Flexible Riser Installation Optimisation Based on Virtual Prototyping. In OCEANS 2019-Marseille (pp. 1-6). IEEE.

Owen, D.G., Qin, K., 1986. Model Tests and Analysis of Flexible Riser Systems In:Proceedings of the 5th International Conference on Offshore Mechanics and Arctic Engineering, Tokyo.

Pedersen, P. T., 2015. Marine structures: future trends and the role of universities.Engineering,1(1), 131-138.

Ruan W, Bai Y, Yuan S. , 2017. Dynamic analysis of unbonded flexible pipe with bend stiffener constraint and bending hysteretic behavior. Ocean Engineering, 130: 583-596.

Ranket Manual, 2012. [accessed 2020 March 20]. http://raknet.com/raknet/manual/

Systemes D., 2019. ABAQUS Users' Guide 2019. Dassault Systemes: Paris, France.

Unity User Manual, 2019. [accessed 2020 March 20] https://docs.unity3d.com/Manual/index.html

Wang, F., Chen, J., Gao, S., Tang, K., & Meng, X. , 2017. Development and sea trial of real-time offshore pipeline installation monitoring system. Ocean Engineering, 146, 468-476.

Yu Y, Duan M, Sun C, Zhong Z, Liu H. 2017. A virtual reality simulation for coordination and interaction based on dynamics calculation, Ships and Offshore Structures, 12:6, p. 873-884

Zhang X, Duan M, Mao D, Yu Y, Yu J & Wang Y. 2017. A mathematical model of virtual simulation for deepwater installation of subsea production facilities, Ships and Offshore Structures, 12:2, p.182-195